# Noise performance of phase-insensitive multicasting in multi-stage parametric mixers

**Christopher K. Huynh,[1,2,*] Zhi Tong,[1] Evgeny Myslivets,[1] Andreas O. J. Wiberg,[1] James R. Adleman,[2] Sanja Zlatanovic,[2] Everett W. Jacobs,[2] and Stojan Radic[1]**

[1]*Department of Electrical and Computer Engineering, University of California, San Diego, La Jolla, California 92093, USA*

[2]*Space and Naval Warfare Systems Center Pacific, San Diego, California 92152, USA*

[*]*christopher.huynh@navy.mil*

**Abstract:** Noise properties of large-count spectral multicasting in a phase-insensitive parametric mixer were investigated. Scalable multicasting was achieved using two-tone continuous-wave seeded mixers capable of generating more than 20 frequency non-degenerate copies. The mixer was constructed using a multistage architecture to simultaneously manage high Figure-of-Merit frequency generation and suppress noise generation. The performance was characterized by measuring the conversion efficiency and noise figure of all signal copies. Minimum noise figure of 8.09dB was measured. Experimental findings confirm that noise of the multicasted signal does not grow linearly with copy count and that it can be suppressed below this limit.



**OCIS codes:** (190.4410) Nonlinear optics, parametric processes; (270.2500) Fluctuations, relaxations, and noise.

## References and links

1. T. Okuno, M. Hirano, T. Kato, M. Shigematsu, and M. Onishi, "Highly nonlinear and perfectly dispersion-flattened fibres for efficient optical signal processing applications," Electron. Lett. **39**(13), 972–974 (2003).
2. E. Myslivets, B. P. Kuo, N. Alic, and S. Radic, "Generation of wideband frequency combs by continuous-wave seeding of multistage mixers with synthesized dispersion," Opt. Express **20**(3), 3331–3344 (2012).
3. R. H. Stolen and J. E. Bjorkholm, "Parametric amplification and frequency conversion in optical fibers," IEEE J. Quantum Electron. **18**(7), 1062–1072 (1982).
4. Z. Tong, A. O. J. Wiberg, E. Myslivets, B. P. P. Kuo, N. Alic, and S. Radic, "Spectral linewidth preservation in parametric frequency combs seeded by dual pumps," Opt. Express **20**(16), 17610–17619 (2012).
5. C.-S. Bres, A. O. J. Wiberg, B. P.-P. Kuo, N. Alic, and S. Radic, "Wavelength multicasting of 320-Gb/s channel in self-seeded parametric amplifier," IEEE Photon. Technol. Lett. **21**(14), 1002–1004 (2009).
6. F. S. Yang, M. C. Ho, M. E. Marhic, and L. G. Kazovsky, "Demonstration of two-pump fibre optical parametric amplification," Electron. Lett. **33**(21), 1812–1813 (1997).
7. J. M. C. Boggio, P. Dainese, and H. L. Fragnito, "Performance of a two-pump fiber optical parametric amplifier in a 10 Gb/s x 64 channel dense wavelength division multiplexing system," Opt. Commun. **218**(4-6), 303–310 (2003).
8. B. P. P. Kuo, E. Myslivets, N. Alic, and S. Radic, "Wavelength multicasting via frequency comb generation in a bandwidth-enhanced fiber optical parametric mixer," J. Lightwave Technol. **29**(23), 3515–3522 (2011).
9. A. O. J. Wiberg, Z. Tong, L. Liu, J. L. Ponsetto, V. Ataie, E. Myslivets, N. Alic, and S. Radic, "Demonstration of parallel polychromatic sampling based analog-to-digital conversion at 8GS/s," in CLEO: 2012 – Science and Innovations, OSA Technical Digest (online) (Optical Society of America, 2012), paper CM2B.5.
10. C.-S. Bres, S. Zlatanovic, A. O. J. Wiberg, J. R. Adleman, C. K. Huynh, E. W. Jacobs, J. M. Kvavle, and S. Radic, "Parametric photonic channelized RF receiver," IEEE Photon. Technol. Lett. **23**(6), 344–346 (2011).
11. J. Kvavle, J. Adleman, C. Huynh, C. Bres, S. Zlatanovic, A. Wiberg, B. Kuo, E. Myslivets, S. Radic, and E. Jacobs, "Optical domain wideband RF spectrum analysis using parametric mixing," in *CLEO: 2011 - Laser Applications to Photonic Applications*, OSA Technical Digest (CD) (Optical Society of America, 2011), paper CThR3.
12. S. Radic, "Parametric Signal Processing," IEEE J. Sel. Top. Quantum Electron. **18**(2), 670–680 (2012).
13. C. J. McKinstrie, S. Radic, and M. G. Raymer, "Quantum noise properties of parametric amplifiers driven by two pump waves," Opt. Express **12**(21), 5037–5066 (2004).
14. C. J. McKinstrie, S. Radic, and A. R. Chraplyvy, "Parametric amplifiers driven by two pump waves," IEEE J. Sel. Top. Quantum Electron. **8**(3), 538–547 (2002) (and references therein).

#179022 - $15.00 USD Received 1 Nov 2012; revised 14 Dec 2012; accepted 15 Dec 2012; published 8 Jan 2013

# Report Documentation Page

*Form Approved*
*OMB No. 0704-0188*



| 1. REPORT DATE | 2. REPORT TYPE | 3. DATES COVERED |
|---|---|---|
| **08 JAN 2013** | | **00-00-2013 to 00-00-2013** |

| 4. TITLE AND SUBTITLE | 5a. CONTRACT NUMBER |
|---|---|
| **Noise performance of phase-insensitive multicasting in multi-stage parametric mixers** | 5b. GRANT NUMBER |
| | 5c. PROGRAM ELEMENT NUMBER |
| 6. AUTHOR(S) | 5d. PROJECT NUMBER |
| | 5e. TASK NUMBER |
| | 5f. WORK UNIT NUMBER |
| 7. PERFORMING ORGANIZATION NAME(S) AND ADDRESS(ES) **Space and Naval Warfare Systems Center Pacific,San Diego,CA,92152** | 8. PERFORMING ORGANIZATION REPORT NUMBER |
| 9. SPONSORING/MONITORING AGENCY NAME(S) AND ADDRESS(ES) | 10. SPONSOR/MONITOR'S ACRONYM(S) |
| | 11. SPONSOR/MONITOR'S REPORT NUMBER(S) |

12. DISTRIBUTION/AVAILABILITY STATEMENT
**Approved for public release; distribution unlimited**

13. SUPPLEMENTARY NOTES
**OPTICS EXPRESS, Vol. 21, No. 1, 14 January 2013**

14. ABSTRACT
**Noise properties of large-count spectral multicasting in a phaseinsensitive parametric mixer were investigated. Scalable multicasting was achieved using two-tone continuous-wave seeded mixers capable of generating more than 20 frequency non-degenerate copies. The mixer was constructed using a multistage architecture to simultaneously manage high Figure-of-Merit frequency generation and suppress noise generation. The performance was characterized by measuring the conversion efficiency and noise figure of all signal copies. Minimum noise figure of 8.09dB was measured. Experimental findings confirm that noise of the multicasted signal does not grow linearly with copy count and that it can be suppressed below this limit.**

15. SUBJECT TERMS

| 16. SECURITY CLASSIFICATION OF: | | | 17. LIMITATION OF ABSTRACT | 18. NUMBER OF PAGES | 19a. NAME OF RESPONSIBLE PERSON |
|---|---|---|---|---|---|
| a. REPORT | b. ABSTRACT | c. THIS PAGE | | | |
| **unclassified** | **unclassified** | **unclassified** | **Same as Report (SAR)** | **12** | |

15. P. Kylemark, P. O. Hedekvist, H. Sunnerud, M. Karlsson, and P. A. Andrekson, "Noise characteristics of fiber optical parametric amplifiers," J. Lightwave Technol. **22**(2), 409–416 (2004).
16. P. L. Voss, R. Tang, and P. Kumar, "Measurement of the photon statistics and the noise figure of a fiber-optic parametric amplifier," Opt. Lett. **28**(7), 549–551 (2003).
17. P. O. Hedekvist and P. A. Anderson, "Noise characteristics of fiber-based optical phase conjugators," J. Lightwave Technol. **17**(1), 74–79 (1999).
18. P. Kylemark, J. Ren, M. Karlsson, S. Radic, C. J. McKinstrie, and P. A. Andrekson, "Noise in dual-pumped fiber-optical parametric amplifiers: theory and experiments," J. Lightwave Technol. **25**(9), 2837–2846 (2007).
19. K. K. Y. Wong, K. Shimizu, M. E. Marhic, K. Uesaka, G. Kalogerakis, and L. G. Kazovsky, "Continuous-wave fiber optical parametric wavelength converter with +40-dB conversion efficiency and a 3.8-dB noise figure," Opt. Lett. **28**(9), 692–694 (2003).
20. Z. Tong, A. O. J. Wiberg, N. Alic, and S. Radic, "Noise performance of an eight-sideband parametric mixer," in *Optical Fiber Communication Conference and Exposition (OFC/NFOEC), 2012 and the National Fiber Optic Engineers Conference*, pp.1–3, 4–8 March 2012.
21. Z. Tong, A. O. J. Wiberg, E. Myslivets, B. P. P. Kuo, N. Alic, and S. Radic, "Broadband parametric multicasting via four-mode phase-sensitive interaction," Opt. Express **20**(17), 19363–19373 (2012).
22. G. P. Agrawal, *Nonlinear fiber optics* 4th ed. (Academic, 2007).
23. C. J. McKinstrie, M. Karlsson, and Z. Tong, "Field-quadrature and photon-number correlations produced by parametric processes," Opt. Express **18**(19), 19792–19823 (2010).
24. Z. Tong, A. Bogris, C. Lundström, C. J. McKinstrie, M. Vasilyev, M. Karlsson, and P. A. Andrekson, "Modeling and measurement of the noise figure of a cascaded non-degenerate phase-sensitive parametric amplifier," Opt. Express **18**(14), 14820–14835 (2010).
25. C. J. McKinstrie, M. Yu, M. G. Raymer, and S. Radic, "Quantum noise properties of parametric processes," Opt. Express **13**(13), 4986–5012 (2005).
26. Z. Tong, C. Lundström, P. A. Andrekson, C. J. McKinstrie, M. Karlsson, D. J. Blessing, E. Tipsuwannakul, B. J. Puttnam, H. Toda, and L. Grüner-Nielsen, "Towards ultrasensitive optical links enabled by low-noise phase-sensitive amplifiers," Nat. Photonics **5**(7), 430–436 (2011).
27. M. V. Vasilyev, "Distributed phase-sensitive amplification," Opt. Express **13**(19), 7563–7571 (2005).
28. S. Radic and C. J. McKinstrie, "Two-pump fiber parametric amplifiers," Opt. Fiber Technol. **9**(1), 7–23 (2003).
29. E. Myslivets and S. Radic, "Advanced fiber optic parametric synthesis and characterization," in *Optical Fiber Communication Conference,* OSA Technical Digest (CD) (Optical Society of America, 2011), paper OWL5.
30. E. Myslivets, C. Lundström, J. M. Aparicio, S. Moro, A. O. J. Wiberg, C.-S. Bres, N. Alic, P. A. Andrekson, and S. Radic, "Spatial equalization of zero-dispersion wavelength profiles in nonlinear fibers," IEEE Photon. Technol. Lett. **21**(24), 1807–1809 (2009).
31. Z. Tong, A. Bogris, M. Karlsson, and P. A. Andrekson, "Full characterization of the signal and idler noise figure spectra in single-pumped fiber optical parametric amplifiers," Opt. Express **18**(3), 2884–2893 (2010).

## 1. Introduction

Recent advances in highly nonlinear fiber (HNLF) [1] have allowed for precise control of the dispersive and nonlinear properties necessary for efficient four-wave mixing (FWM) in multistage parametric devices [2]. Seeded by two continuous-wave (CW) dither-less pumps [3], three-stage mixers were used to demonstrate a 150 nm wide frequency comb with high optical signal-to-noise ratio (OSNR) [2,4] and tunable frequency pitch. Many-tone parametric exchanges in a cavity-less, single-pass structure were used in the past to stimulate a large number of spectrally-shifted replicas (i.e. optical sidebands) of digital signals with net-positive gain, low distortion and negligible jitter [5]. Spectrally uninhibited signal replication was subsequently used to demonstrate parametric amplification [6,7], errorless broadcasting [8], polychromatic sampling [9], variable-resolution optical domain RF channelization [5,10,11] and sub-rate electronic pre-processors [12].

The performance of wideband multicasting mixers has been characterized in terms of signal conversion efficiency (CE), bit error rate (BER) and linearity [8,9]. The CE considered here is defined as the ratio between the copy and the original signal powers. The noise properties of parametric multicasting with high sideband count is another important measure, and is commonly characterized by noise figure (NF) measured as the ratio of the input signal OSNR and the OSNR of a selected copy. Noise characteristics of parametric processes have been extensively studied when the sideband count is low and has been recently reviewed by McKinstrie [13,14]. Unlike the well-studied two-sideband [15–17] and four-sideband devices [14,18] which correspond to 3 dB [19] and 6 dB [13] NF limits respectively, the noise performance of a many-sideband parametric mixer has not yet been the subject of systematic

#179022 - $15.00 USD Received 1 Nov 2012; revised 14 Dec 2012; accepted 15 Dec 2012; published 8 Jan 2013

study. As explained by McKinstrie [13], NF will increase with the sideband count when phase matching conditions are met, where parametric photon exchange comprehensively couples vacuum fluctuations from all equally participating sideband frequencies. By increasing sideband generation, it is reasonable to expect that more noise photons will be generated at any sideband frequency, thus raising the NF for the entire device. In practice, phase matching within the mixer is neither achromatic nor spatially constant, preventing uninhibited coupling between all generated sidebands. A recent measurement [20] of an eight-sideband parametric multicaster indicated approximately 10 dB NF—in agreement with the theoretical prediction resting in achromatic noise coupling [13]. The mixer in this measurement used a short 64 m HNLF section, allowing for nearly ideal, broadband phase matching encompassing all eight sidebands. However, an efficient mixer is expected to be both longer and able to generate many more sidebands, limiting the relevance of the reported measurement [20]. Consequently, this paper addresses this critical question: how does the noise scale in a many-sideband parametric mixer operating under physically feasible phase matching conditions? The answer to this question is fundamentally important for understanding the physics and ultimate performance limits of devices relying on generation of many frequency non-degenerate signal copies.

While an analytical description for frequency conversion has been extensively studied [3,13–15,18], a similar description of many-sideband parametric exchange poses significant challenge as the number of participating waves scales rapidly with number of generating (higher-order) pumps [2,8,12]. While the analytic solution indeed might be articulated in the future, it is plausible that such description will not be scalable with sideband count. Consequently, we have characterized the noise performance of a wideband phase-insensitive (PI) parametric multicaster by combined numerical and experimental study. Furthermore, the results of this study could have critical implications for phase-sensitive parametric many-copy multicasters [21].

This paper is organized in four sections. Section 2 introduces the general principle used for broadband phase-insensitive multicasting. Section 3 describes the numerical study of many-sideband parametric process and reports its results. Section 4 details the experimental setup and observed measurements. The last section summarizes the results and discusses the practical and basic implications of the study.

## 2. Principle of CW-seeded multi-stage parametric multicasting

A simplified version of the multistage parametric mixer architecture that was recently used to generate wideband, variable-pitch frequency comb from two CW pump seeds [2] is shown in Fig. 1. The pump-pump beat is considered here as a fully modulated sinusoid which evolves into a pulse train with repetition rate directly controlled by the pump seed frequency separation ( $\Delta f$ ). This evolution is driven by spectral broadening and frequency selective chirp of the harmonically modulated input through self-phase modulation (SPM) in the first stage HNLF segment with linear dispersion slope. The chirp value is governed by the nonlinear figure of merit (NFOM), defined by the product of the nonlinear HNLF parameter ($\gamma$), peak input power ($P$) and the effective interaction length ($L$). L in practice differs little from the physical HNLF length due to low fiber loss. The position of the HNLF zero dispersion wavelength (ZDW) is critically important: pulse generation should not be accomplished in the anomalous dispersion regime. This regime allows for an exponential gain which enables excessive vacuum noise amplification and subsequent OSNR loss [22]. ZDW tuning allows for a simple mechanism for noise control in the first stage [2]. Therefore a ZDW is chosen such that both pump waves experience normal dispersion, preventing unnecessary vacuum noise amplification.

The NFOM of the entire (multi-stage) mixer system must be optimized to achieve efficient frequency generation, with pump power and fiber length being the most practical design variables. However, one cannot choose *any* pump power or use excessive fiber length:

#179022 - $15.00 USD Received 1 Nov 2012; revised 14 Dec 2012; accepted 15 Dec 2012; published 8 Jan 2013

high pump power generally implies lower OSNR while longer HNLF requires more precise local dispersion control over the distributed mixing process. A device designed with very high NFOM is not necessarily the optimal choice as it can suffer from higher order nonlinear effects that will destabilize and ultimately destroy the seed pulse for efficient frequency generation. The effects of instability-mediated pulse destruction and its impact on intra-mixer peak power are illustrated in Fig. 2. Furthermore, pulse destabilization negatively impacts practical design of the compressor stage because it causes the peak pulse power to fluctuate rapidly with respect to the compressor length as in Fig. 2(A). Indeed, pulse distortion driven by third order dispersion (TOD) was identified as one such destructive mechanism [22].

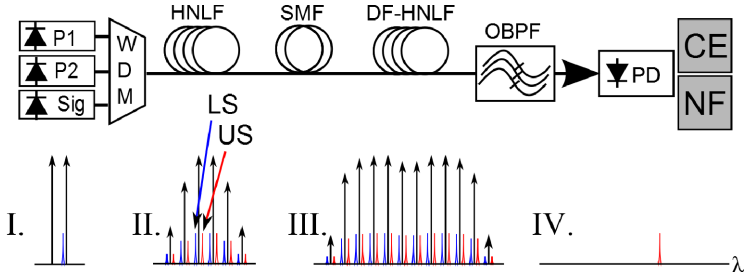


Fig. 1. The three stage architecture begins with launching two pump waves (black) with the signal (I) into the first stage HNLF. The system is spectrally broadened in this first stage (II), temporally compressed in the single mode fiber (SMF) stage, and injected into the second HNLF stage consisting of dispersion flattened HNLF (DF-HNLF). The DF-HNLF stage generates a comb and multicasts the signal (III). The sideband of interest can then be filtered by an optical bandpass filter (OBPF) and detected (IV). Processing of the detected signal resolves the CE and NF, referenced against the input signal. Red and blue signals correspond respectively to lower sidebands (LS) and upper sidebands (US) as referenced later in the text.

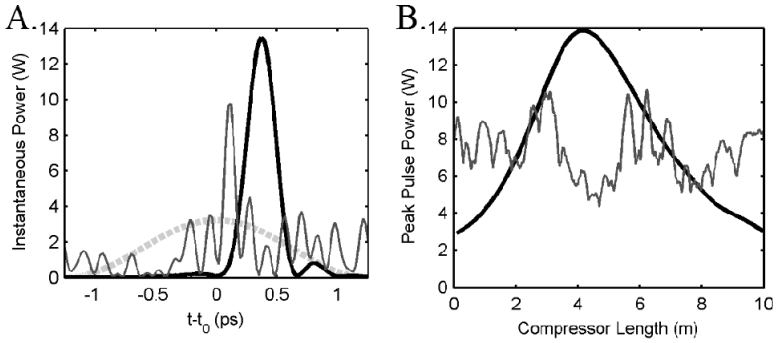


Fig. 2. **A.** The original sinusoid (grey dotted curve) is formed after combining two pump seeds and a signal. Maximally compressed pulses are formed after 105 m HNLF section in the first mixer stage and 4.0 m of SMF in the second, compression stage (heavy solid curve). An attempt to induce higher chirp in longer (300 m HNLF) first stage matched by a 2.96 m SMF compression (light solid curve) leads to effective pulse loss via strong TOD distortion. **B.** Pulse peak power evolution within the SMF compressor is shown for the 105 m (heavy solid curve) and the 300 m (light solid curve) long first stage.

Excessive NFOM in the first stage causes pulse distortion which results in lower multicasting efficiency in the compressive stage.

The compressive stage re-aligns the phases of the frequency elements of the chirped pulse in order to achieve high pulse compression and peak pulse power. Standard single mode fiber (SMF) has sufficiently large dispersion to perform the compression process within a few meters of interaction. Pulse distortion caused by a combination of higher order dispersion and ZDW fluctuations in the fiber ultimately limit the compression ratio as precise, high-order

#179022 - $15.00 USD Received 1 Nov 2012; revised 14 Dec 2012; accepted 15 Dec 2012; published 8 Jan 2013

dispersion control, not available in a conventional SMF compressor, is needed to achieve Fourier-limited pulse compression. The SMF compressor length can be approximated by [2]:

$$L_C = \frac{t_0^2}{|\beta_2|}\frac{|C|}{\left(1+C^2\right)} \tag{1}$$

where $t_0 = 0.59/2\Delta f$ and $C = 2\gamma PL(0.59\pi)^2$ are the characteristic time and chirp parameter, and $\beta_2$ is the second-order dispersion of the compressive fiber. This formula is derived as a first-order approximation governed by the NFOM of the preceding stage. Given the parameters used to generate well behaved compression in Fig. 2, $L_C$ can be calculated to be 1.9 m with nonlinear parameter (γ) of 18.5 $W^{-1}km^{-1}$, individual pump power (P) of 1 W, HNLF length (L) of 105 m, pump frequency separation ($\Delta f$) of 400 GHz, and $\beta_2$ of $2\cdot10^{-26}$ $s^2/m$. The analytical approximation has better accuracy in slow compression regimes shown by Myslivets [2]. In this case, the simulation suggests that the approximation will provide for less than half the peak compression power available in SMF. A more insightful compressor length can be calculated numerically using a non-linear Schrödinger equation (NLSE) description of the multi-tone parametric process.

We have been able to substantially improve the performance of the compression stage by using a NLSE-driven multicaster design. This approach has allowed for stable pulse

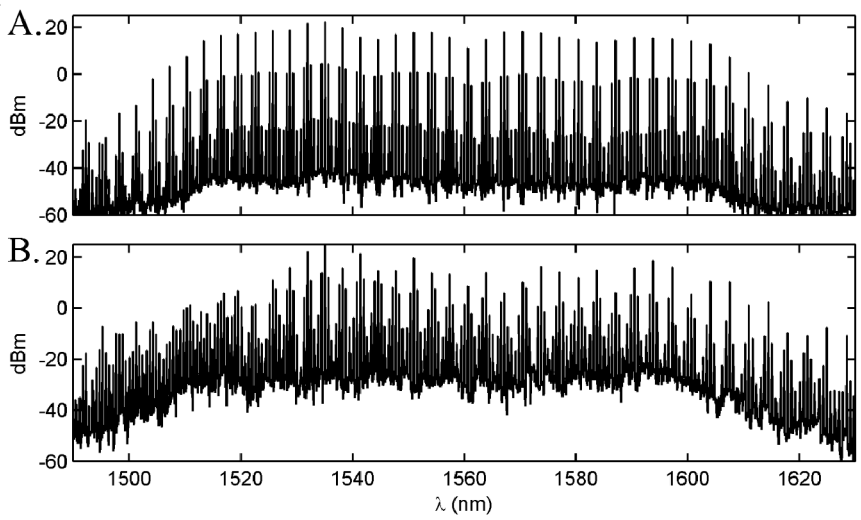


Fig. 3. NLSE-designed three-stage mixer with pumps at 1547.7 nm and 1550.9 nm and signal at 1548.3 nm. **A.** Near -optimal comb generation using 105 m HNLF, 4.0 m SMF and 240 m DF-HNLF (with peak dispersion of –0.15 ps/nm·km at 1565 nm). **B.** Sub-optimal comb generation corresponding to distorted pulse regime with mixer stages corresponding to 300 m HNLF, 2.96 m SMF, and 240 m DF-HNLF.

generation with peaks exceeding 10 W, improving the frequency generation efficiency of the third mixer stage. The compressed pulse is then injected into a dispersion flattened HNLF (DF-HNLF), possessing negatively parabolic dispersion with approximately flat dispersion in the comb generation band. Figure 3 illustrates the drastic differences between the optimally designed compressor stage and that of suboptimal generation corresponding to compressor-induced pulse breakup (Fig. 2).

It should be noted here that we reference idler modes as sidebands to an adjacent pump as an analogy to RF sidebands about an RF carrier. Sidebands with higher wavelength than the pump wavelength are called upper sidebands (US) here, unlike in RF systems where the

#179022 - $15.00 USD Received 1 Nov 2012; revised 14 Dec 2012; accepted 15 Dec 2012; published 8 Jan 2013

nomenclature is derived in the frequency domain. Likewise a lower wavelength to the nearby pump is a lower sideband (LS). This distinction is illustrated in Fig. 1, and provides a descriptive framework that will be used shortly.

### 3. Simulation procedure and numerical results

The noise performance of a three-stage parametric mixer was simulated using an adaptive-step NLSE solver. The NLSE numerical model was configured to simulate a signal-ASE dominated semi-classical model previously shown to be in agreement with the quantum description by McKinstrie [23] and Tong [24]. The agreement suggests that a fiber optical parametric amplifier (FOPA) model can be generalized to characterize wideband spectrally multicasted signals created in many-frequency interactions. The physical parameters for all three stages of the mixer were adapted in correspondence to the practical fibers that were available and matched the mixer requirements described by Myslivets [2]. Such requirements are driven by the pump seed frequencies and desired mixer operation.

The first nonlinear stage used a standard (linear dispersive slope) HNLF that had a ZDW at 1556 nm, a $\gamma$ of 18.5 $W^{-1}km^{-1}$ and a dispersion slope of 0.021 $ps/nm^2 \cdot km$, with seed pumps positioned within the normal dispersion regime. The compressor stage was a segment of SMF with 0.06 $ps/nm^2 \cdot km$ dispersion slope. Since the compressor length is determined by the NFOM of the system preceding it, a lookup table was generated based on the seed pump powers, pump spacing, and the length of the first HNLF stage. For high NFOM and large pump spacing, the phase matching conditions produced highly unstable compression (Fig. 2). Under the condition of unstable pulse compression, the instantaneous peak power can change by multiple watts over half a meter of SMF without attaining a large compression ratio, undermining the practical realization of the system. The second nonlinear stage used DF-HNLF with negatively parabolic dispersion, with peak chosen for normal and anomalous operational regimes. The first case corresponded to the dispersion peak of −0.15 ps/nm·km at 1565 nm, guaranteeing normal dispersion across the entire operational band of interest. For anomalous comb generation, peak dispersion was + 0.05 ps/nm·km at 1565 nm with ZDWs at 1524 nm and 1605 nm.

Two pump wavelengths were placed at 1547.7 nm and 1550.9 nm, each with 29 dBm optical power injected into the mixer. A −5 dBm, shot-noise limited signal at a 1548.3 nm center wavelength was launched concurrently with the pump seeds producing a signal-pump frequency spacing of 75 GHz. The mixer was assumed to operate in correlated-phase regime [4], allowing for the selection of narrow-linewidth lasers throughout the numerical simulation procedure. All waves were assumed to be co-polarized and polarization mode dispersion (PMD) was neglected, in agreement with very low PMD parameters of all fiber types used in experiment. Quantum noise (vacuum fluctuations) was modeled as an additive Gaussian white noise at the mixer input, characterized by signal noise $n_s$ photons with $\langle n_s \rangle = 0$ and $\langle |n_s|^2 \rangle = h\nu_s / 2$, where $\langle \cdot \rangle$ denotes the expectation operation; $h$ is Planck's constant and $\nu_s$ is the optical frequency of the signal [25]. The signal or multi-casted signal copy output was filtered with a 0.4 nm (50 GHz) optical filter, then detected with a fast (12.5 GHz) square-law photodetector exhibiting a 4th order Butterworth filter response. Using the known signal input power, the linear CE and NF were calculated as follows [26]:

$$CE = \bar{I}_{out} / \rho P_{in} \tag{2}$$

$$NF = \frac{1}{G} + \frac{P_{in}(S_{out} - S_{in})}{2h\nu \bar{I}_{out}^{\,2} B} \tag{3}$$

#179022 - $15.00 USD Received 1 Nov 2012; revised 14 Dec 2012; accepted 15 Dec 2012; published 8 Jan 2013

where $P_{in}$ is the input signal power, $\rho$ is the responsivity of the photodetector, $\bar{I}_{out}$ is the average output photocurrent of the signal copy of interest, $S_{out}$ and $S_{in}$ are the output and input photocurrent variances respectively, and B is the bandwidth of the receiver. Without any excess noise input, $S_{in}$ refers to the shot noise.

Careful consideration was paid to ensure enough data points were collected to reduce uncertainty in the simulation data. First, the simulation time window was chosen such that a minimum of 64 points could be sampled within the bandwidth of our simulated detector, reducing time-window dependent NF fluctuations to under 0.1 dB. Second, the simulations were averaged using 100 ensemble members, each with an independent, randomly generated seed for each laser phase. Finally, the NLSE parametric mixer model and noise calculation were compared against the well-known result [15] of a single pump FOPA expressing 3 dB NF and showed excellent agreement in spectral and temporal domains. The simulation results provided useful insight in frequency comb evolution within the mixer. As the pump pulse propagates along the HNLF and DF-HNLF, the frequency comb broadens with high fidelity (low noise) if a normal dispersion regime is chosen. In this case, idler sidebands can be increased to achieve net-positive conversion efficiency. Figure 4 shows a broad perspective of multicasted sideband characteristics under combs generated under normal dispersion and anomalous dispersion. Figure 4(A) shows the NF and CE of a three-stage mixer composed of 105 m HNLF, 4.0 m SMF, and 240 m DF-HNLF, corresponding to the case described in Section 2. Most of the net-positive CE region has a NF of 7.4-10.9 dB. The NF tends to >13 dB near the spectral edge of the net-positive CE region as a result of lower CE, which extends into a net-loss regime. The minimum NF of about 7.4 dB may suggest phase insensitive operation similar to a two pump FOPA [13,26,27]. The oscillation-like behavior seen near the band edges are indicative of decoupling between the upper and the lower idler sidebands: upper sidebands are generated more efficiently than the lower sidebands at the higher wavelength (lower frequency) edge whereas the converse is true at the lower wavelength (higher frequency) edge. This type of conversion oscillation has been observed earlier by Kvavle [11]. The sidebands with this type of preferential gain show improved NF at <12 dB even with CE as low as −7 dB and suggest a mechanism for suppressing the NF even further for a specific subset of bands.

When the DF-HNLF is simulated with seed pumps centered in anomalous dispersion, the pump depletes at the center of the comb band, and the noise performance becomes worse as seen in Fig. 4(B). Under this regime, parametric amplification can be dominated by modulation instability with exponential gain [28]. As the spectral center of the comb has higher NFOM, these regions undergo more rapid pump depletion thereby lowering the CE of

#179022 - $15.00 USD Received 1 Nov 2012; revised 14 Dec 2012; accepted 15 Dec 2012; published 8 Jan 2013

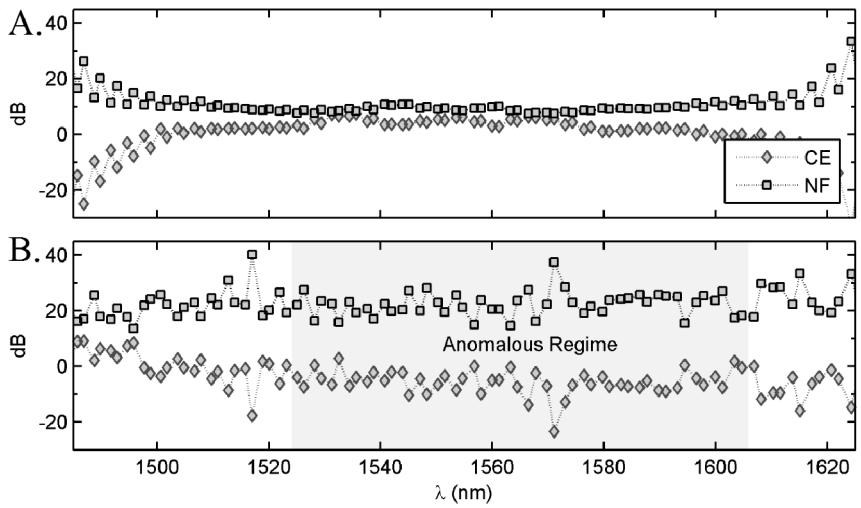


Fig. 4. **A.** The CE and NF for a simulated parametric multi-casting mixer with 105 m in first stage HNLF, a 4.0 m SMF compressor, and 240 m of DF-HNLF. This fiber system was seeded with 1547.7 nm and 1550.9 nm ideal 29 dBm pumps and a −5 dBm signal laser. The CE shows 100 nm of net positive gain operation. The NF at the center of this regime is 7.4-10.9 dB and < 13 dB near the edge of transparent operation. **B.** When the multicaster operates in anomalous dispersion (DF-HNLF with peak dispersion at 0.05 ps/nm·km), net-gain is lost to pump depletion.

nearby sideband copies. The anomalous case is particularly instructive as it illustrates such rapid depletion by driving the frequency comb center into net-loss CE. Even in bands outside the anomalous region where the sidebands enjoy CE as high as 10 dB, the NF remains above 10 dB. Consequently, this example of anomalous comb generation presents a strong argument for selecting mode seeds under a normal dispersion regime when low-noise frequency comb generation is of interest.

## 4. Experimental setup and results

The three-stage parametric experimental setup was constructed with parameters closely matching the simulation architecture; the practical setup is shown in Fig. 5. The two lasers centered at 1547.7 nm and 1550.9 nm and used as pump seeds were injection locked to a master oscillator in order to guarantee linewidth preservation and improved OSNR during higher-order tone generation [4]. After injection locking, the slave lasers were near shot-limited with 20 dBm output. They were then amplified and sent through 0.4 nm (50 GHz) wide filters before being combined to achieve 29.2 dBm and 29.0 dBm powers respectively prior to injection into the parametric mixer with a signal wave. The signal wave was a near shot-limited free running signal laser with −4 dBm power centered at 1548.3 nm. Each wave polarization was adjusted to achieve a co-polarized state at the launch point into the mixer. The first stage mixer was constructed using 105 m of HNLF with ZDW at 1554 nm and 0.021 ps/nm$^2$·km dispersion slope and $\gamma$ at 22 W$^{-1}$km$^{-1}$. The SMF compressor length was 4 m. The second nonlinear stage was built using a 240 m long DF-HNLF and was manufactured with dispersion variations below 1 ps/nm·km over the comb bandwidth. Optical couplers with 1% tapping ratio were placed before and after the mixer to measure return power, indicative of stimulated Brillouin scattering (SBS) onset and to monitor the comb with an OSA.

#179022 - $15.00 USD Received 1 Nov 2012; revised 14 Dec 2012; accepted 15 Dec 2012; published 8 Jan 2013

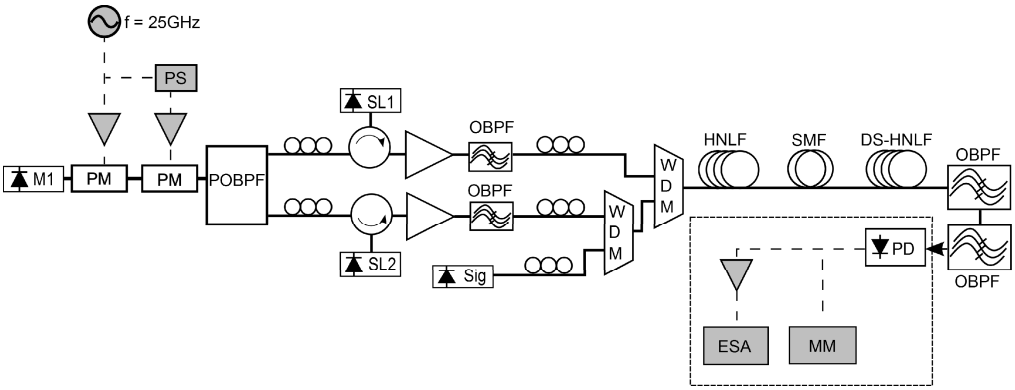


Fig. 5. The dual-pumped parametric multi-caster was set up with two injection locked CW lasers SL1 and SL2 to generate a 3.2 nm (400 GHz) pitch comb. The injection locking was referenced to a narrow linewidth master CW laser M1 through a 0.2 nm (25 GHz) pitch comb generated by a pair of phase modulators (PM). The locking lines were selected by a programmable OBPF (POBPF). A separate CW signal laser was combined with the two pumps and injected into the mixer system. The output was filtered optically to broadly reject the comb and again to narrowly select the band of interest for detection and CE and NF calculation. The electronic processing was performed with a multi-meter (MM) and electrical spectrum analyzer (ESA).

The nonlinear fibers were spliced to the SMF compressor stage and to the rest of the experimental architecture such that the cumulative mixer loss (SMF input to SMF output) was 2.5 dB. A tailored splicing technique was used for four SMF/HNLF interfaces with typical loss under 0.5 dB per interface. The low estimated fiber loss substantiates the effective length assumption made under simulations. Fiber tensioning [29] was employed to simultaneously control the fiber dispersion profile of each nonlinear stage and increase the SBS threshold. Specifically, the first HNLF section was longitudinally strained, increasing its SBS threshold to beyond 30 dBm [30]. The dispersion of the DF-HNLF was precisely adjusted by applying constant longitudinal tension to shift the dispersion into normal regime, which suppresses modulation instability and associated noise [2,8]. The SBS was negligible in all experiments in spite of high NFOM [22] due to tensioning in the HNLF stage and spectral broadening in the DF-HNLF stage.

The generated comb was subsequently filtered using two stages. The first filter rejected all pump frequencies through a 0.6 nm (75 GHz) wide thin-film bandpass device. The second filter selected a 0.4 nm (50 GHz) optical band rejecting all out-of band contributions to below the measurement noise floor. The filtering process was monitored by an OSA at 0.1 nm resolution bandwidth. The selected signal was then detected, and the noise was measured using an electrical spectrum analyzer (ESA) and subsequently averaged using 64 samples. To measure the output noise, the detected signal had to be electrically amplified above the ESA noise floor (Fig. 5). The photocurrent was monitored using a multi-meter (MM) and served to calibrate the shot noise of the selected copy against that of the input signal [4,31].

The simulated and measured CE and NF are shown in Fig. 6, and are in general agreement. The measured results exhibit 8-12 dB NF in C-band (1535 nm to 1565 nm) while maintaining net-positive CE. The simulation predicted NF to be 8.32-10.88 dB in this region. The opposite curvatures of simulated and measured NF were attributed to spectrally localized phase matching processes not accounted for in the simulation; the same mechanism may also

#179022 - $15.00 USD Received 1 Nov 2012; revised 14 Dec 2012; accepted 15 Dec 2012; published 8 Jan 2013

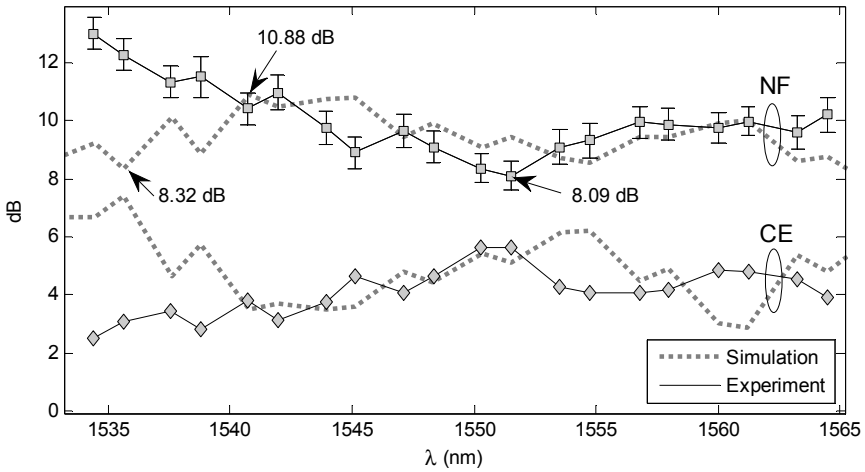


Fig. 6. CE and NF comparison between simulation of a near-optimal case (Section 3) and experiment. Simulation shows CE to be between 2 to 8 dB with a NF from 8.32 dB to 10.88 dB. The post DF-HNLF measurement shows net positive CE across 30 nm and NF less than 10 dB across 20 nm culminating in a minimum NF of 8.09 dB with maximum error +/– 0.6 dB.

contribute to comb generation over a narrower band than predicted. The experiment showed over 30 nm of net-positive multicasting operation with a minimum NF of 8.09 dB. While the measured NF minima was predicted by the simulation model, the multicasting bandwidth was smaller than the simulated 100 nm wide comb because the fibers used in the experiment were specifically selected for low NF rather than high-count sideband generation. More significantly, the dispersion fluctuations in the HNLF and DF-HNLF were not considered in simulation, underscoring the importance of precise, *spatially local dispersive control* [2]. To date, there are no known characterization techniques to locally probe the dispersion profile of DF-HNLF with sufficient resolution, pointing to an obvious direction for further research.

Within C-Band (30 nm), 20 sidebands were generated with net-positive CE. Achromatic vacuum noise coupling and spectrally uniform mixing [13] are expected to support uninhibited, linear scaling of NF with sideband count. It is straightforward to predict a NF in excess of 13 dB under this paradigm. When expanded beyond C-band, such reasoning predicts a NF of 17.8 dB when 60 sidebands are generated as illustrated by our simulation. While the numerical model in this paper assumes spatially homogeneous phase-matching conditions, the simulated NF minimum (7.4 dB) remains more than 10 dB lower than what would be predicted under achromatic coupling. Indeed, neither the model nor measurements support the achromatic mixing hypothesis which calls for progressively larger NF as the sideband count grows. Instead, the results suggest that only spectrally close modes contribute significantly to noise generation in this mixer architecture. Sidebands at the outer spectral edge of the frequency comb possess low CE and may not contribute significantly to the mixing process within C-Band, and were neglected from noise coupling considerations [13].

## 5. Conclusion

The noise properties of net-positive spectral multicasting within C-Band were analyzed and experimentally characterized. We described important design principles governing the compressor length and intra-stage dispersion parameters supporting this process. Both length and dispersion were shown to have a direct and measurable effect on the fidelity of the multicast sidebands. The measured and simulated results indicate that high-count sideband spectral replication cannot be reconciled with the noise generation prediction using an achromatic coupling model [13], which assumes that ideal phase matching is maintained over

#179022 - $15.00 USD Received 1 Nov 2012; revised 14 Dec 2012; accepted 15 Dec 2012; published 8 Jan 2013

the entire operational bandwidth. The observed mixer behavior suggests that sideband interactions are not governed in a spectrally global manner such that each sideband interacts with all other sidebands equally. Instead, the report indicates that a multistage design can be used to exercise spectral localization of the mixing process, where spectrally close sideband interactions dominate. In this regime, a minimal NF of 8.09 dB was measured. While the experiment clearly points to a practical path towards low-NF multicasting, the model still needs improvement by incorporating spatially local dispersion fluctuation behavior as a result of accurate characterization of DF-HNLF. It is important to note, however, that both model and measurement confirm that noise generation does not scale linearly with increasing sideband numbers and that sideband-count-scaled noise generation can be optimized with the mixer design. While important for PI devices, the result also has critical implications for the phase-sensitive (PS) counterpart recently studied in a many-copy regime [21]. The reported study shows that low-noise signal replication may be practically attainable and ultimately independent of total copy count, *if a combination of an ideal, local phase-matching and waveform shaping can be achieved in a single device*. This particular finding points to a viable path for realizing high fidelity, high-count parametric spectral multicasting that has no equivalent in conventional frequency non-degenerate signal replication.

**Acknowledgments**

The work reported hereunder was supported by the Office of Naval Research (ONR) Discovery and Invention (D&I) Program and Naval Innovative Science and Engineering (NISE) Program at SPAWAR Systems Center Pacific. The authors graciously acknowledge Sumitomo Electric Industries for providing the HNLF and DF-HNLF used in this work.

#179022 - $15.00 USD Received 1 Nov 2012; revised 14 Dec 2012; accepted 15 Dec 2012; published 8 Jan 2013